THESIS FOR THE DEGREE OF LICENTIATE OF ENGINEERING IN THERMO AND FLUID DYNAMICS

Waste Heat Recovery in Heavy Duty Diesel Engines

Thermodynamic Potential of Rankine and Flash Cycles for Low and High Temperature Heat Sources

JELMER RIJPKEMA

Department of Mechanics and Maritime Sciences,
Division of Combustion and Propulsion Systems
CHALMERS UNIVERSITY OF TECHNOLOGY

Gothenburg, Sweden 2018

Waste Heat Recovery in Heavy Duty Diesel Engines
Thermodynamic Potential of Rankine and Flash Cycles for Low and High Temperature Heat Sources
JELMER RIJPKEMA

Thesis for the degree of Licentiate of Engineering 2018:18
Department of Mechanics and Maritime Sciences,
Division of Combustion and Propulsion Systems
Chalmers University of Technology
SE-412 96 Gothenburg
Sweden
Telephone: +46 (0)31-772 1000

Chalmers Reproservice
Gothenburg, Sweden 2018

Waste Heat Recovery in Heavy Duty Diesel Engines
Thermodynamic Potential of Rankine and Flash Cycles for Low and High Temperature Heat Sources
Thesis for the degree of Licentiate of Engineering in Thermo and Fluid Dynamics
JELMER RIJPKEMA
Department of Mechanics and Maritime Sciences,
Division of Combustion and Propulsion Systems
Chalmers University of Technology

Abstract

Over 50% of the energy released by burning fuel in a truck engine is lost as heat rather than being used to propel the vehicle. A promising method for capturing and reusing this heat, and thereby improving engine efficiency, is to exploit thermodynamic cycles for waste heat recovery (WHR). The goal of this thesis is to evaluate the thermodynamic performance of multiple thermodynamic cycles using many different working fluids, considering all relevant low- and high-temperature heat sources available in a heavy duty Diesel engine to be able to identify the best possible combination of heat source, working fluid and thermodynamic cycle. To evaluate the potential of each heat source, the operating conditions of a real heavy duty Diesel engine were used to define boundary conditions. A GT-Power model of such an engine was previously developed and experimentally validated for the stationary points of the European stationary cycle (ESC). Using the results from this model, an energy and exergy analysis was performed, which revealed four heat sources with the potential for waste heat recovery: the charge air cooler (CAC), the coolant flow, the exhaust gas recirculation cooler (EGRC), and the exhaust flow. Modelica models were developed for four different thermodynamic cycles: the organic Rankine cycle (ORC), the transcritical Rankine cycle (TRC), the trilateral flash cycle (TFC), and the organic flash cycle (OFC). Simulations with different boundary conditions, constraints, and engine operating conditions showed that variation in these conditions significantly affected the results obtained. In general, the best WHR performance was achieved when the thermal profiles of heat source and the chosen thermodynamic cycle were closely matched. Using realistic constraints and boundary conditions, the ORC gave the best performance with acetone, cyclopentane, or methanol as the working fluid. However, taking flammability and toxicity into account, the best-performing fluids were R1233zd(E), MM, and Novec649.

Keywords: Waste Heat Recovery; Internal Combustion Engines; Heavy Duty Diesel Engine; Organic Rankine Cycle; Transcritical Rankine Cycle; Trilateral Flash Cycle; Organic Flash Cycle

List of publications

This thesis is based on the work contained in the following publications:

Publication I Rijpkema, J., Munch, K., Andersson, S.B., *Thermodynamic Potential of Rankine and Flash Cycles for Waste Heat Recovery in a Heavy Duty Diesel Engine,* Energy Procedia 2017;129:746-753, doi:10.1016/j.egypro.2017.09.110.

Publication II Rijpkema, J., Andersson, S.B., and Munch, K., *Thermodynamic Cycle and Working Fluid Selection for Waste Heat Recovery in a Heavy Duty Diesel Engine,* SAE Technical Paper 2018-01-1371, 2018, doi:10.4271/2018-01-1371.

Acknowledgements

Let me start by thanking my two supervisors, Karin Munch and Sven B. Andersson. Ever since our first meeting via Skype, they have made me feel at ease and this feeling has never left me throughout my PhD studies. Their sincere and personal interest in me, and their professional attitude and guidance concerning my work and project, have allowed me to work with a clear mind and a free heart.

My thanks also go out to all lab personnel, whose support is invaluable and who make working in the lab one of the most pleasant parts of my PhD studies. I want to especially thank Anders Mattsson, who I consider to be the living example of an engineer - someone who can build everything from anything. It is a pleasure to work with him and learn from him. More thanks goes out to the administrative officers at the department, who make the administrative tasks so much easier. Also important to me is the opportunity to collaborate with industrial partners through our working group. I want to express my gratitude to all involved, and especially to Ingemar Denbratt, our project leader, as well as Arne Andersson, Fredrik Ekström, Henrik Salsing, and Olof Erlandsson for their time, our fruitful collaborations and their excellent support. I am also thankful to the Swedish Energy Agency, whose funding made this research and thesis possible.

Of course, my life as a PhD student in Sweden would not have been the same without my colleagues from the Combustion Division. Common activities, politically incorrect jokes, informal fikas that sometimes last for hours, and perhaps more importantly, our regular after-works, make our division the best at Chalmers. A special thanks goes out to my roommate, Marco, who has the ability to connect with everybody he meets and, if he manages to stop talking, is actually a good listener (except when it comes to music). It is great to have a roommate who shares similar ideas about life and relationships, so thank you for the good conversations and discussions.

This thesis would not be possible without my parents, whose infinite support has brought me to where I am today. I also would not be who I am without the important people in my life: my brother and his girlfriend, Douwe and Jule, and my little niece Lea as well as my extended family (Ron, Anne, Jeroen, Vincent and Aimée), and my friends, who live all over the world. My deepest thanks and love go to my girlfriend, Marleen, who was the first to support my choice for starting my PhD studies. Her love and care allow me to focus on my work, while making sure that I do not forget about the finer things in life. Thank you, moppie, for being there for me and making sure that wherever we live, I have not a house, but a home to come to.

Contents

Nomenclature

h	specific enthalpy, J/kg
$\dot{m}$	mass flow rate, kg/s
p	pressure, Pa
$\dot{Q}$	heat transfer rate, W
s	specific entropy, J/kg/K
T	temperature, K
$\overline{T}$	mean temperature, K
$\dot{W}$	power, W
x	vapor mass fraction
$\dot{X}$	exergy rate, W

Greek symbols

η	efficiency
Π_{P}	pressure ratio

Subscripts

0	reference state
c	cycle
con	condensation / condenser
ev	evaporation / evaporator
eng	engine
exp	expander
fv	flash vessel
is	isentropic
liq	liquid
mxr	mixer
pmp	pump
pp	pinch point
sat	saturation / saturated
si	sink
so	source
sup	superheating
tv	throttling valve
vap	vapor

Abbreviations

CAC	charge air cooler
EATS	exhaust aftertreatment system
EGR	exhaust gas recirculation
EGRC	exhaust gas recirculation cooler
ESC	European stationary cycle
GHG	greenhouse gas
GWP	global warming potential
ODP	ozone depletion potential
OFC	organic flash cycle
ORC	organic Rankine cycle
SFC	single flash cycle
TFC	trilateral flash cycle
TRC	transcritical Rankine cycle
WHR	waste heat recovery

1 Introduction

1.1 Background

There is a scientific consensus that human activity is the dominant cause of the observed warming of the planet since the mid-20th century. This increase in the average global temperature has several physical consequences, including warming of the atmosphere and the ocean, diminishing snow and ice cover, and rising sea levels. The warming is attributed to an increase in greenhouse gas (GHG) emissions in the atmosphere, which is typically quantified in units of tonnes of CO_2 equivalent [1]. Figure 1.1 shows the relative contributions of of different economic sectors to the European Union's overall GHG emissions (on the left) and the contributions for the different transport sectors (on the right) [2].

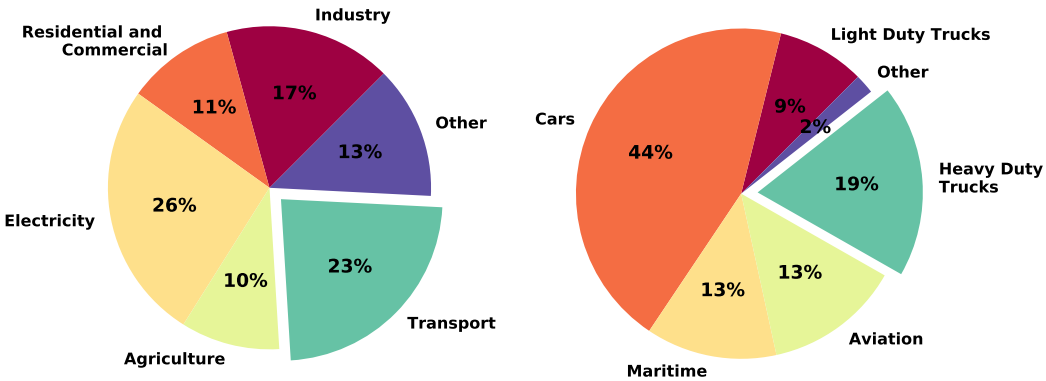

Figure 1.1: *Relative contributions to GHG emissions per economic sector (left) and per transport sector (right) in the European Union [2].*

This thesis focuses on the contributions of the heavy duty Diesel engine within the transport sector. Figure 1.1 shows that the transport sector accounts for 23% of the total GHG emissions, and that heavy duty trucks account for 19% of those emissions. Therefore, reducing the GHG emissions of heavy duty trucks could significantly reduce overall GHG emissions. One way to reduce GHG emissions due to heavy duty transport is to improve the efficiency of the engine, because more efficient engines use fossil fuels more efficiently and thus produce less CO_2 per unit of work. The efficiency of heavy duty engines can be increased by implementing a combination of different technologies, including improved combustion strategies, reducing friction and parasitic losses, engine downsizing, engine downspeeding, improving transmission systems, hybridization, turbocompounding, waste heat recovery, and/or improving engine control [3, 4]. This thesis focuses on waste heat recovery; the following sections discuss some of the most important technologies currently available for this purpose.

1.2 Waste Heat Recovery

Research on increasing engine efficiency has been driven by increasingly strict emissions standards and consumer demand for more fuel-efficient vehicles. Waste Heat Recovery (WHR) technologies have attracted considerable interest in this context, especially those based on turbo-compounding, thermo-electric generators, or thermodynamic power cycles [5]. Turbo-compounding, which has been incorporated into commercial aircraft and heavy duty engines, is achieved by placing a turbine downstream of the turbocharger to recover energy from the exhaust. This can reduce fuel consumption by 3-5%, although it may increase fuel consumption at low engine loads by increasing the back pressure. Thermo-electric generators use semiconductor elements to generate an electrical potential based on a temperature gradient. While this approach has the advantages of easy integration into existing vehicles and relatively straightforward control, its low efficiency and comparatively high costs present significant challenges [5, 6].

This thesis focuses on the use of thermodynamic cycles for WHR in automotive applications. Many studies in this field focus on the organic Rankine cycle (ORC) with the exhaust as the heat source [5, 7–9], and have succeeded in reducing fuel consumption by 4 to 8%. Other studies have explored the potential of the exhaust gas recirculation cooler (EGRC) [10–12], either as a separate heat source or in combination with the exhaust, and have achieved similar reductions in fuel consumption (4 to 5%). Greater reductions in fuel consumption (of 4 to 15%) have been achieved by also using the charge air cooler (CAC) or engine coolant as a heat source [13–15].

1.3 Objectives

The objective of this thesis is to evaluate waste heat recovery from every available low- and high-temperature heat source in a heavy duty Diesel engine, considering multiple thermodynamic cycles and working fluids. The WHR potential of each source was initially evaluated, and the results obtained were used to investigate the performance of different combinations of thermodynamic cycle and working fluid when applied to each of the identified heat sources. The overall aim is to identify combinations of heat source, thermodynamic cycle, and working fluid that offer the highest thermodynamic performance for use in automotive systems.

2 Fundamentals

This chapter is divided into three sections, each discussing an aspect of WHR particularly important in automotive applications. The first section discusses the heat sources available in a typical heavy duty Diesel engine, and the second reviews the thermodynamic cycles that can be used for WHR, while the third focuses on the working fluids.

2.1 Heat Sources in Heavy Duty Diesel Engines

A schematic depiction of a heavy duty Diesel engine showing the components relevant for WHR is shown in Fig. 2.1. The inlet air enters the engine and is compressed by the turbocharger compressor, then cooled by the CAC before it enters the cylinders. Fuel is injected into the cylinder and compressed, igniting the fuel-air mixture. Some of the energy released during combustion is transferred to the coolant. After combustion, the exhaust gas leaves the cylinders. A portion of the exhaust gas is cooled in the EGRC, mixed with air, and returned to the cylinders. The remainder is expanded in the turbocharger turbine and leaves the exhaust via the exhaust aftertreatment system (EATS), still containing a substantial amount of useful energy.

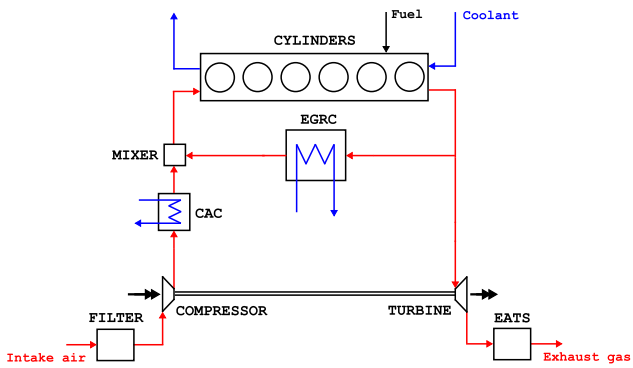

Figure 2.1: *Schematic layout of a heavy duty Diesel engine with a turbocharger and EGR.*

The engine has four main sources of heat loss: two low-temperature sources in the form of the CAC and the engine coolant, and two high-temperature sources in the form of the EGRC and the exhaust gas out. The temperatures and pressures of these sources vary with the engine's load and speed, which depend on the vehicle's requirements. Operating points for heavy duty engines have been defined as part of the European stationary cycle (ESC). The engine speed of a given operating point is indicated by a letter (A, B, or C, corresponding to low, intermediate, and high speed), and the load is represented by a number (25, 50, 75, or 100, corresponding to percentages of the engine's maximum load). Simulations have shown that the dominant operating points in a typical long haul cycle are A25, A50 and A75 [11], as shown in Figure 2.2.

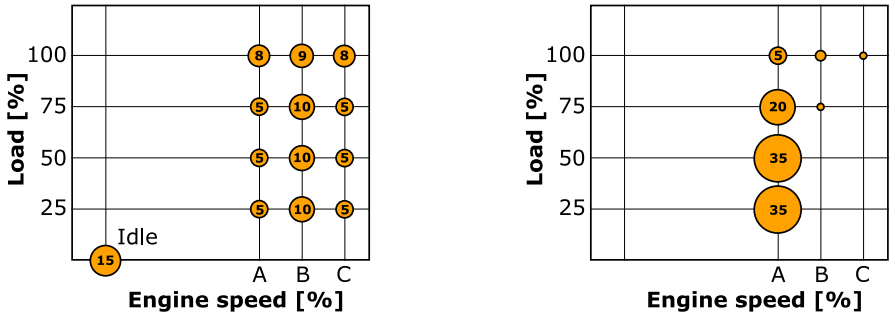

Figure 2.2: *Weightings in percentages of the operating points in the ESC (left) and a typical long haul cycle (right) [11].*

2.2 Thermodynamic Cycles for Waste Heat Recovery

Figure 2.3 shows schematic representations of the organic Rankine cycle (ORC), transcritical Rankine cycle (TRC), trilateral flash cycle (TFC), and organic flash cycle (OFC) and T-s diagrams are shown in Figure 2.4.

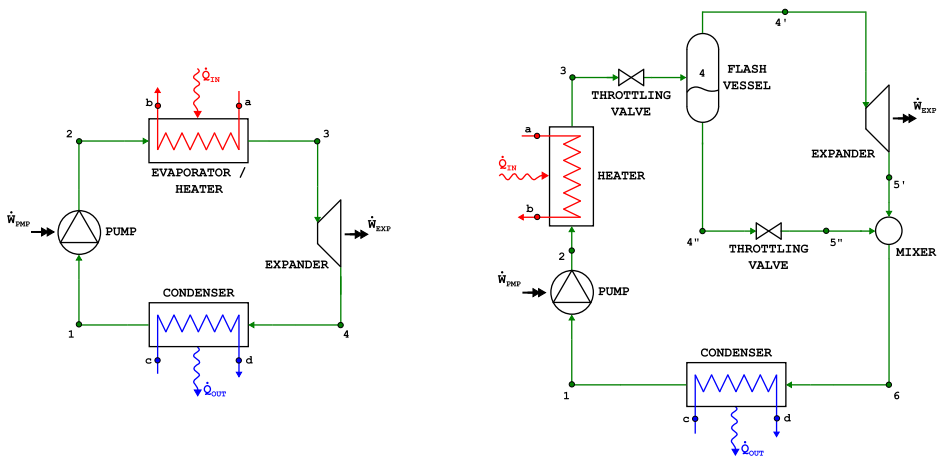

Figure 2.3: *Schematic representations of the ORC, the TRC, the TFC (left) and the OFC (right).*

The ORC, TRC and TFC share the same sequence of steps:

1	→	2:	compression
2	→	3:	evaporation (ORC) / heating (TRC, TFC)
3	→	4:	expansion
4	→	1:	condensation
a	→	b:	heat source flow (EGRC, coolant, exhaust)
c	→	d:	heat sink flow

The ORC and TRC work according to the same principles, except that the maximum pressure in the TRC is above the critical pressure and so no evaporation occurs. The TFC only heats the pressurized liquid up to the saturation point. The expansion is then started from the saturation point, consequently leading to an expanding mixture that is wet, making it difficult to achieve good expander efficiencies. To avoid the challenging wet expansion, the OFC is proposed as an alternative of which the the steps are shown below.

1	→	2:	compression
2	→	3:	heating
3	→	4:	flash expansion
4	→	4':	vapor separation
4'	→	5':	vapor expansion (power production)
4	→	4":	liquid separation
4"	→	5":	liquid expansion
5', 5"	→	6:	mixing
6	→	1:	condensation
a	→	b:	heat source flow (CAC, EGRC, coolant, exhaust)
c	→	d:	heat sink flow

By first flashing to an intermediate pressure, the vapor and liquid can be separated, after which the saturated vapor can be expanded. This avoids wet expansion at the expense of reduced pressure and mass flow, and necessitates the addition of a flash vessel to the circuit. Note that strictly speaking, the ORC is the only cycle that involves evaporation. However, for the sake of convenience and consistency, the high pressure in all four cycles is referred to as the "evaporating pressure" in this thesis.

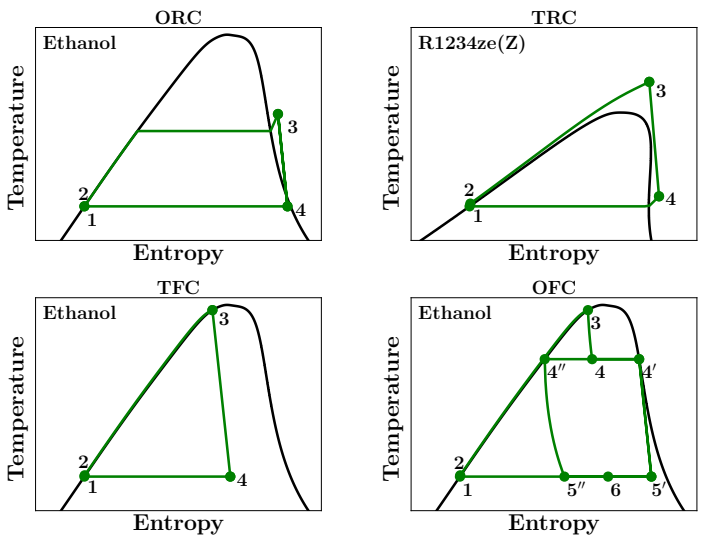

Figure 2.4: *T-s diagrams for the ORC (top left), the TRC (top right), the TFC (bottom left) and the OFC (bottom right) using different working fluids but the same heat source.*

2.3 Working Fluids

A key factor in the design of a thermodynamic power cycle for WHR is the choice of working fluid. The list of possible working fluids is long, encompassing many different fluid classes such as hydrocarbons (HC), perfluorocarbons (PCF), chlorofluorocarbons (CFC, HCFC), hydrofluorocarbons (HFC), hydrofluoroolefins (HFO), ethers, alcohols, siloxanes, and even inorganics (e.g. water). Despite extensive efforts to identify the best performing working fluid, no one candidate has proven to be optimal in all cases. This is mainly due to differences between applications, the working conditions of the studied cycles, the fluids initially chosen for consideration in the different studies, the chosen optimization schemes, and/or the selection criteria that were applied. Several fluid properties have been identified as important in WHR applications [16–18], of which the most relevant are:

Thermodynamic performance: The main criterion is the thermodynamic performance of the working fluid, which is related to a number of interdependent thermodynamic properties such as the critical point, latent and specific heat, density, and boiling temperature. The complexity of this interdependence makes it difficult to predict the best-performing working fluid for any given application.

Shape of the vapor saturation curve: The shape of the saturation curve is typically classified as wet, dry, or isentropic depending on the slope of the saturation vapor curve in the T-s diagram. For wet fluids, superheating is often used to avoid wet conditions at the end of the expansion and to achieve higher power outputs. For isentropic fluids, superheating might be beneficial for the power output, although the effect is small. In contrast, for dry fluids, a high amount of superheating can even be detrimental [16, 17].

Thermal stability: At high temperatures, organic fluids may undergo chemical decomposition, which limits the maximum temperature of the cycle [18]. Although it is difficult to obtain the thermal stability temperature data for many fluids, the maximum temperatures for several hydrocarbons, fluorocompounds, and refrigerants have been estimated to be above 300 °C [19], although lower values of around 250 °C have also been reported [20].

Environmental impact: A working fluid's environmental impact is typically evaluated in terms of two measures: the ozone depletion potential (ODP) and greenhouse warming potential (GWP). Under the Montreal Protocol, CFCs have been phased out over the last few years and HCFCs will be phased out between 2020 and 2030 because of their high ODP values [17]. In the EU, fluorinated greenhouse gases with GWPs higher than 150 are banned from use in air-conditioning systems for passenger cars and light-duty vehicles, and the European Commission is considering extending this ban to other vehicle classes including heavy duty vehicles [12].

Component sizing: This practical criterion is especially important for automotive applications where there is limited space available. The volume flow rate has a direct effect on the sizing of the heat exchangers and expanders. Consequently, working fluids with high vapor densities are preferred [21].

Material compatibility: For practical systems, it is necessary to carefully consider the working fluid's material compatibility in terms of factors such as its corrosiveness and compatibility with seals.

Transport properties: The transport properties of the fluids, such as the viscosity and thermal conductivity, are important thermodynamic properties to consider since they affect the heat transfer and pressure drop characteristics.

Flammability: The flammability of the fluid has important implications for its safety in practical automotive applications.

Health effects: The detrimental effects of the working fluids on health, such as toxicity and carcinogenicity, must be carefully considered when selecting a working fluid.

Availability / Costs: A final important practical consideration is the fluid's availability and cost.

3 Modeling and Methods

The inputs for the cycle simulations were taken from an existing engine model, which is described in the first section of this chapter. This description is followed by a presentation of the mathematical models used to simulate the thermodynamic cycles, and a discussion of the general modeling approach used in the simulations.

3.1 Heavy Duty Diesel Engine

A GT-Power [22] model of a heavy duty Diesel engine was developed during an earlier project at Chalmers [6], which has been experimentally validated for the operating modes of the ESC [23]. The model is based on an engine with the specifications shown in Table 3.1 and a schematic representation shown in Figure 3.1.

Table 3.1: Heavy duty Diesel engine specifications.

Type:	Volvo D13 US	Compression ratio:	16.0:1
Configuration:	4 stroke / 6 cylinder in line / EGR	Bore x Stroke:	131 x 158 mm
Peak power:	500 hp (373 kW)	Displacement:	12.8 L
Peak torque:	1750 lb-ft (2373 Nm)	Aspiration:	Turbocharged

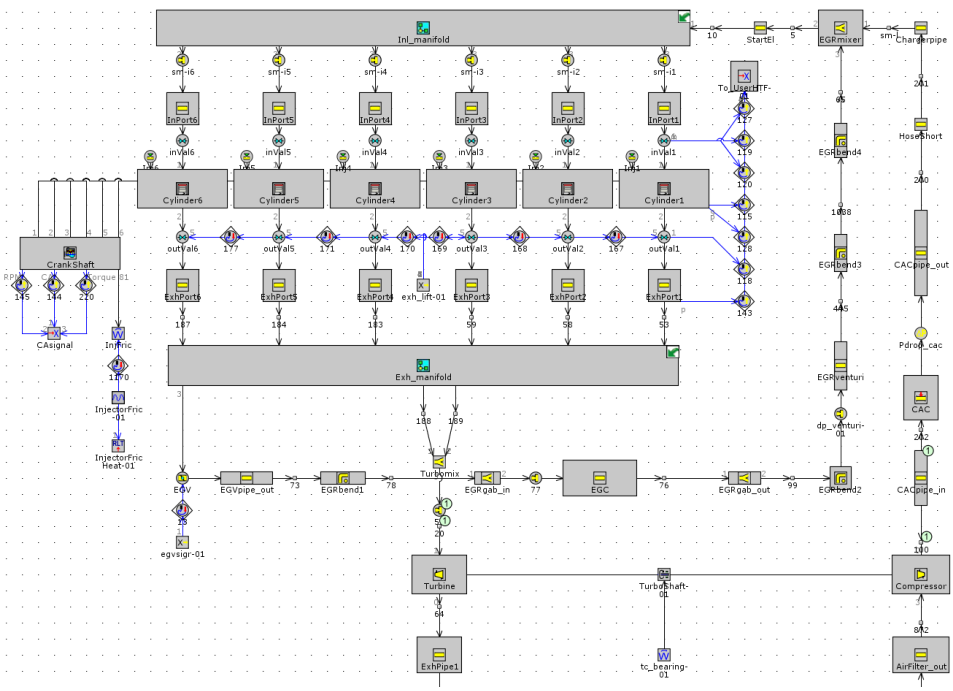

Figure 3.1: *GT Power Model of the Volvo D13 Engine*

The temperatures, pressures and mass flows from the model results served as input for the thermodynamic cycle simulations. To be able to evaluate not only the quantity, but also the quality of the energy flows, these were converted to exergy flows using Eq. (3.1), which takes into account the mean temperature level ($\overline{T}$) at which the energy is available as well as the reference temperature (T_0) [24].

$$\dot{X}_{\text{loss}} = \dot{Q}_{\text{loss}} \frac{\overline{T} - T_0}{\overline{T}} \tag{3.1}$$

Two different expressions were used to determine the mean temperatures ($\overline{T}$), depending on the source: for heat exchangers Eq. (3.2) was used based on the enthalpy (h) and entropy (s) differences, while for the flow devices Eq. (3.3) was used [24].

$$\text{Heat exchanger:} \quad \overline{T} = \frac{h_{\text{out}} - h_{\text{in}}}{s_{\text{out}} - s_{\text{in}}} \tag{3.2}$$

$$\text{Compressor, turbine:} \quad \overline{T} = \frac{T_{\text{in}} + T_{\text{out}}}{2} \tag{3.3}$$

3.2 Thermodynamic Cycles

The thermodynamic cycle models were built using the Modelica [25] programming language and modeled by decomposing the cycles into individual components connected by nodes. Each node contains the thermodynamic state, which includes all of the fluid's thermodynamic properties and is defined by two independent properties (pressure and enthalpy in most cases). Mathematical descriptions of each cycle and component are given below. All of the components were modeled using the following assumptions:

- The system is in a steady state
- There are no pressure losses in the system, including the heat exchangers and piping
- There are no heat losses to the environment
- Changes in kinetic and potential energy can be neglected
- Expansion in the throttling valves is isenthalpic
- There is perfect mixing and separation of the working fluids
- The isentropic efficiencies of the pump and expander are constant

3.2.1 Cycles

The following section presents mathematical descriptions of each individual component in the thermodynamic cycles. The heat transferred from the source to the cycle depends on the source outlet temperature, which is either a fixed value or dependent on the pinch point. If the heat input into the cycle and the cycle pressure are known, one extra equation is needed to close the system of equations. The necessary equation depends on the type of cycle under consideration, as shown below. For reference, schematic depictions of the circuits for each cycle can be found in Figure 2.3.

Organic Rankine Cycle
The ORC offers four possibilities for closing the system of equations. Either by setting the saturated vapor condition at the evaporator outlet or condenser inlet by defining the enthalpy at the outlet or inlet ($h_{\mathrm{ev,out}}$ or $h_{\mathrm{con,in}}$) as the saturated vapor condition ($h_{\mathrm{sat,vap}}$) at the corresponding pressure ($p_{\mathrm{ev,out}}$ or $p_{\mathrm{con,in}}$). Or by setting the superheated temperature ($T_{\mathrm{ev,out}}$ or $T_{\mathrm{con,in}}$) at the corresponding saturation temperature (T_{sat}) by adding a specified degree of superheating (ΔT_{sup}). This can be expressed in four equations, of which only one can be defined in the cycle simulations:

$$\begin{cases} h_{\mathrm{ev,out}} = h_{\mathrm{sat,vap}} @\ p_{\mathrm{ev,out}} & \text{Saturated vapor at evaporator outlet} \\ h_{\mathrm{con,in}} = h_{\mathrm{sat,vap}} @\ p_{\mathrm{con,in}} & \text{Saturated vapor at condenser inlet} \\ T_{\mathrm{ev,out}} = T_{\mathrm{sat,ev}} + \Delta T_{\mathrm{sup,ev}} & \text{Superheated temperature at evaporator outlet} \\ T_{\mathrm{con,in}} = T_{\mathrm{sat,con}} + \Delta T_{\mathrm{sup,con}} & \text{Superheated temperature at condenser inlet} \end{cases}$$

Transcritical Rankine Cycle
Since no evaporation occurs in the TRC, it is not possible to set the conditions at the evaporator outlet. Therefore, either the saturated vapor condition at the condenser inlet ($h_{\mathrm{con,in}}$) is set as the saturated vapor condition ($h_{\mathrm{sat,vap}}$) at the condenser pressure ($p_{\mathrm{con,in}}$). Or the superheated temperature ($T_{\mathrm{con,in}}$) at the condenser inlet is set by adding a specified degree of superheating (ΔT_{sup}) to the saturation temperature at the condenser pressure ($T_{\mathrm{con,in}}$). These conditions can be expressed mathematically using the following equations:

$$\begin{cases} h_{\mathrm{con,in}} = h_{\mathrm{sat,vap}} @\ p_{\mathrm{con,in}} & \text{Saturated vapor at condenser inlet} \\ T_{\mathrm{con,in}} = T_{\mathrm{sat,con}} + \Delta T_{\mathrm{sup,con}} & \text{Superheated temperature at condenser inlet} \end{cases}$$

Trilateral Flash Cycle
For the TFC, there is only one condition at the evaporator outlet: saturated liquid at the outlet of the evaporator. Therefore, the enthalpy at the outlet of the evaporator ($h_{\mathrm{ev,out}}$) is set to the saturated liquid enthalpy ($h_{\mathrm{sat,liq}}$) at the evaporator pressure ($p_{\mathrm{ev,out}}$), mathematically expressed below.

$$h_{\mathrm{ev,out}} = h_{\mathrm{sat,liq}} @\ p_{\mathrm{ev,out}} \quad \text{Saturated liquid at evaporator outlet}$$

Organic Flash Cycle
As with the TFC, the enthalpy at the outlet of the evaporator ($h_{\mathrm{ev,out}}$) in the OFC is set to the saturated liquid enthalpy ($h_{\mathrm{sat,liq}}$) at the evaporator pressure ($p_{\mathrm{ev,out}}$). An additional equation is needed to calculate the intermediate pressure at the flash vessel inlet ($p_{\mathrm{fv,in}}$) where a fixed value for the pressure ratio (Π_{P}) is used.

$$h_{\mathrm{ev,out}} = h_{\mathrm{sat,liq}}@\ p_{\mathrm{ev,out}} \quad \text{Saturated liquid at evaporator outlet}$$

$$p_{\mathrm{fv,in}} = p_{\mathrm{pmp,in}} + \frac{p_{\mathrm{ev,out}} - p_{\mathrm{pmp,in}}}{\Pi_{\mathrm{P}}} \quad \text{Intermediate pressure}$$

3.2.2 Components

Each component is connected to other components using nodes that contain the thermodynamic state of the working fluid. Each component is defined by a number of fixed conditions, which are set initially and do not change. Additionally, the component is defined by a set of equations which is simultaneously solved for all components. The fixed conditions and equations for all cycle components are specified below.

3.2.2.1 Pump

Since the condensation temperature is set, either by the minimum pressure or temperature constraint, the pressure at the pump inlet ($p_{\mathrm{pmp,in}}$) is known. Saturated liquid at the pump inlet is assumed ($x_{\mathrm{pmp,in}} = 0$) and the isentropic efficiency of the pump ($\eta_{\mathrm{is,pmp}}$) is set to a fixed value. The pump outlet pressure ($p_{\mathrm{pmp,out}}$) is equal to the evaporating pressure, which is either set or calculated as described in Section 3.2.1. Knowing this pressure, the isentropic and actual enthalpy at the pump outlet (Eq. (3.4) and (3.5)) can be calculated, allowing for the determination of the power required by the pump (Eq. (3.6)).

Fixed conditions:

$$p_{\mathrm{pmp,in}},\ x_{\mathrm{pmp,in}},\ \eta_{\mathrm{is,pmp}}$$

Equations:

$$h_{\mathrm{is,pmp}} = h(p_{\mathrm{pmp,out}},\ s_{\mathrm{pmp,in}}) \tag{3.4}$$

$$h_{\mathrm{pmp,out}} = h_{\mathrm{pmp,in}} + \frac{h_{\mathrm{is,pmp}} - h_{\mathrm{pmp,in}}}{\eta_{\mathrm{is,pmp}}} \tag{3.5}$$

$$\dot{W}_{\mathrm{pmp}} = \dot{m}_{\mathrm{c}}(h_{\mathrm{pmp,out}} - h_{\mathrm{pmp,in}}) \tag{3.6}$$

3.2.2.2 Heat Exchangers

In the cycle simulations, different types of heat exchangers are used: an evaporator/heater and a condenser. In this section, only the evaporator/heater is described, but the equations are the same, although rearranged, for the condenser, and the equations for both types are shown below.

The inlet conditions for the heat source are given ($\dot{m}_{\mathrm{so}},\ p_{\mathrm{so,in}},\ T_{\mathrm{so,in}}$) and using the assumption that there is no pressure loss, the source outlet pressure ($p_{\mathrm{so,out}}$) is known as well. The minimum required temperature difference at the pinch point ($\Delta T_{\mathrm{pp,so}}$) is set as a constraint, where the location of the pinch point varies, depending on where the limiting temperature difference occurs. The total heat transfer from the source (Eq. (3.9)) is the combination of the heat transfer from the source inlet to the pinch point location and from the pinch point to the source outlet (Eq. (3.7 and (3.8)). No heat losses are assumed so the heat transfer from the source is equal to the heat input into the cycle (Eq. (3.10) and (3.11)), which are defined in Eq. (3.12) and (3.13).

Evaporator/Heater

Fixed conditions:

$$\dot{m}_{\mathrm{so}},\ p_{\mathrm{so,in}},\ p_{\mathrm{so,out}},\ T_{\mathrm{so,in}},\ \Delta T_{\mathrm{pp,so}}$$

Equations:

$$\dot{Q}_{\mathrm{pp,so,in}} = \dot{m}_{\mathrm{so}}(h_{\mathrm{so,in}} - h_{\mathrm{pp,so}}) \tag{3.7}$$

$$\dot{Q}_{\mathrm{pp,so,out}} = \dot{m}_{\mathrm{so}}(h_{\mathrm{pp,so}} - h_{\mathrm{so,out}}) \tag{3.8}$$

$$\dot{Q}_{\mathrm{so}} = \dot{Q}_{\mathrm{so,pp,in}} + \dot{Q}_{\mathrm{so,pp,out}} \tag{3.9}$$

$$\dot{Q}_{\mathrm{ev}} = \dot{Q}_{\mathrm{so}} \tag{3.10}$$

$$\dot{Q}_{\mathrm{pp,ev,in}} = \dot{Q}_{\mathrm{so,pp,out}} \tag{3.11}$$

$$\dot{Q}_{\mathrm{ev}} = \dot{m}_{\mathrm{c}}(h_{\mathrm{ev,out}} - h_{\mathrm{ev,in}}) \tag{3.12}$$

$$\dot{Q}_{\mathrm{pp,ev,in}} = \dot{m}_{\mathrm{c}}(h_{\mathrm{pp,ev}} - h_{\mathrm{ev,in}}) \tag{3.13}$$

Condenser

Fixed conditions:

$$\dot{m}_{\mathrm{si}},\ p_{\mathrm{si,in}},\ p_{\mathrm{si,out}},\ T_{\mathrm{si,in}},\ \Delta T_{\mathrm{pp,si}},\ p_{\mathrm{con,in}},\ p_{\mathrm{con,out}},\ x_{\mathrm{con,out}}$$

Equations:

$$\dot{Q}_{\mathrm{pp,si,in}} = \dot{m}_{\mathrm{si}}(h_{\mathrm{pp,si}} - h_{\mathrm{si,in}}) \tag{3.14}$$

$$\dot{Q}_{\mathrm{pp,si,out}} = \dot{m}_{\mathrm{si}}(h_{\mathrm{si,out}} - h_{\mathrm{pp,si}}) \tag{3.15}$$

$$\dot{Q}_{\mathrm{si}} = \dot{Q}_{\mathrm{si,pp,in}} + \dot{Q}_{\mathrm{si,pp,out}} \tag{3.16}$$

$$\dot{Q}_{\mathrm{con}} = \dot{Q}_{\mathrm{si}} \tag{3.17}$$

$$\dot{Q}_{\mathrm{pp,con,in}} = \dot{Q}_{\mathrm{si,pp,out}} \tag{3.18}$$

$$\dot{Q}_{\mathrm{con}} = \dot{m}_{\mathrm{c}}(h_{\mathrm{con,in}} - h_{\mathrm{con,out}}) \tag{3.19}$$

$$\dot{Q}_{\mathrm{pp,con,in}} = \dot{m}_{\mathrm{c}}(h_{\mathrm{con,in}} - h_{\mathrm{pp,con}}) \tag{3.20}$$

3.2.2.3 Expander

The isentropic efficiency of the expander ($\eta_{\text{is,exp}}$) is set with a fixed value, and the expander outlet pressure ($p_{\text{exp,out}}$) is equal to the condensation pressure, which is known. Consequently, the isentropic and actual enthalpy at the expander outlet (Eq. (3.21) and (3.22)) can be calculated, allowing for the determination of the power required by the expander (Eq. (3.23)).

Fixed conditions:

$$p_{\text{exp,out}},\ \eta_{\text{is,exp}}$$

Equations:

$$h_{\text{is,exp}} = h(p_{\text{exp,out}},\ s_{\text{exp,in}}) \tag{3.21}$$

$$h_{\text{exp,out}} = h_{\text{exp,in}} - \eta_{\text{is,exp}}(h_{\text{exp,in}} - h_{\text{is,exp}}) \tag{3.22}$$

$$\dot{W}_{\text{exp}} = \dot{m}_{\text{c}}(h_{\text{exp,in}} - h_{\text{exp,out}}) \tag{3.23}$$

3.2.2.4 Flash Vessel

The pressure at the vessel inlet ($p_{\text{fv,in}}$) is obtained as described in Section 3.2.1. With the thermodynamic properties at the inlet known, the saturated liquid and vapor enthalpies can be calculated (Eq. (3.24) and (3.25)), as well as the mass flows (Eq. (3.26) and (3.27)).

Equations:

$$h_{\text{fv,out,liq}} = h_{\text{sat,liq}}@\ p_{\text{fv,in}} \tag{3.24}$$

$$h_{\text{fv,out,vap}} = h_{\text{sat,vap}}@\ p_{\text{fv,in}} \tag{3.25}$$

$$\dot{m}_{\text{fv,out,liq}} = (1 - x_{\text{fv,in}})\dot{m}_{\text{c}} \tag{3.26}$$

$$\dot{m}_{\text{fv,out,vap}} = x_{\text{fv,in}}\dot{m}_{\text{c}} \tag{3.27}$$

3.2.2.5 Throttling Valve

The throttling valve is assumed to be isenthalpic (Eq. (3.28)), so once the pressures in the system are known or calculated, the thermodynamic properties at the outlet are known.

Equations:

$$h_{\text{tv,out}} = h_{\text{tv,in}} \tag{3.28}$$

3.2.2.6 Mixer

With the mixer at condensing pressure and the assumption of no pressure loss, the inlet and outlet pressures of the mixer ($p_{\text{mxr,in}}$ and $p_{\text{mxr,out}}$) are known. Since perfect mixing is assumed, the outlet mass and energy flows are given by the sum of all the inlet quantities (Eq. (3.29) and (3.30)).

Fixed conditions:

$$p_{\text{mxr,in}},\ p_{\text{mxr,out}}$$

Equations:

$$\dot{m}_{\mathrm{mxr,out}} = \sum_{i=1}^{n} \dot{m}_{\mathrm{mxr,i,in}} \tag{3.29}$$

$$(\dot{m}h)_{\mathrm{mxr,out}} = \sum_{i=1}^{n} (\dot{m}h)_{\mathrm{mxr,i,in}} \tag{3.30}$$

3.3 Modeling Approach

The GT-Power model provided the inputs for the cycle models in Modelica. Simulations were performed using the solvers in Dymola [26] connected to the CoolProp database [27] for the thermodynamic properties of the working fluids. Pre- and post-processing of the simulation data were carried out with Python [28]. To evaluate the maximum power output within the given constraints, a constraints check framework was developed, as shown in Figure 3.2. The working fluid and evaporating pressure serve as inputs and the fixed cycle conditions (e.g., p_{con}, T_{con}) are set before starting each simulation. The results of the simulation are evaluated with respect to the constraints (e.g. ΔT_{pp}, ΔT_{sup}). The framework allows for an automated check of the constraints, thereby enabling evaluation of many working fluids and pressures for the different heat sources.

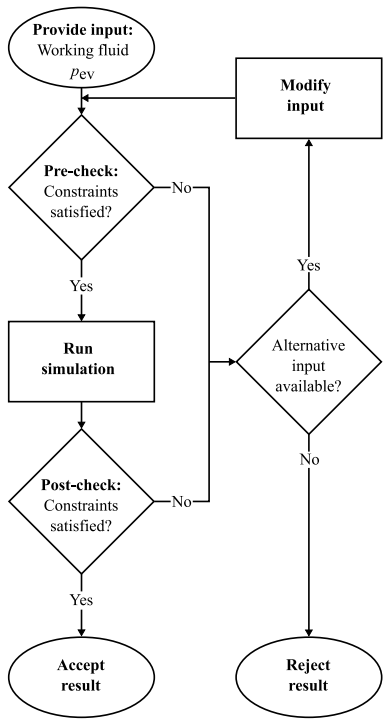

Figure 3.2: *Constraints check framework*

4 Summary of Results

4.1 Paper I

The study presented in *Paper I* had two key objectives: to determine which heat sources inside a heavy duty Diesel engine are suitable for WHR by performing an energy and exergy analysis based on a previously developed GT-Power model, and to identify the combinations of thermodynamic cycles and working fluids that offer the greatest thermodynamic potential for each heat source.

Figure 4.1 shows the ranges of the mass flows and inlet temperatures as well as the energy and exergy losses for the identified heat sources based on the output of the GT-Power model. The figure indicates that all heat sources - CAC, EGRC, coolant, and exhaust - have significant heat and exergy losses, so all four were included in the cycle analysis as potentially useful waste heat sources. A single low speed, intermediate load operating point was selected for further evaluation because it is a dominant operating point in a typical long haul duty cycle [11].

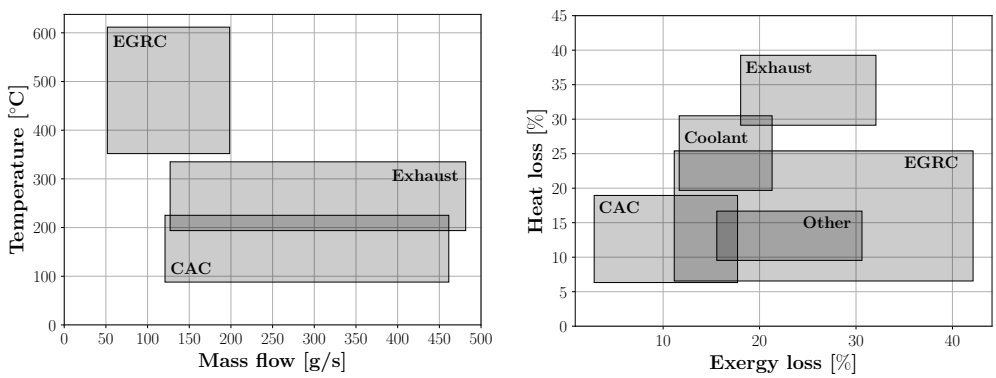

Figure 4.1: *Ranges of mass flows and inlet temperatures (left) and heat and exergy losses (right) for the operating modes from the GT-Power model. All losses are expressed as percentages of the total losses.*

The selected engine operating point provided the operating conditions of each heat source, which served as the input for the simulations of the ORC (defined as RC in the paper), TRC, TFC, and OFC (defined as SFC in the paper). Four working fluids, spanning a range of thermodynamic properties, were selected based on their reported good performance with low- and medium-temperature heat sources [21,29,30]. Bounded by several boundary conditions and constraints, the results for the cycle simulations are shown in Figure 4.2. The TFC and OFC offered the best performance with the CAC as the heat source, regardless of the selected working fluid. The ORC performed especially well with the coolant flow as the heat source, achieving power increases up to 5 kW, again almost independently of the working fluid. Ethanol was the best performing working fluid when the EGRC was used as the heat source, offering a peak power of around 8 kW for both the

ORC and TRC. All cycles achieved similar performance when using the exhaust flow as the heat source, with peak power production of around 5 kW depending on the working fluid. Overall, the results showed that the choice of cycle had the greatest impact on the performance, whereas the different working fluids all performed comparably in most cases. This can be attributed to thermal matching: a better thermal match leads to an increased evaporator outlet temperature, giving better thermodynamic performance.

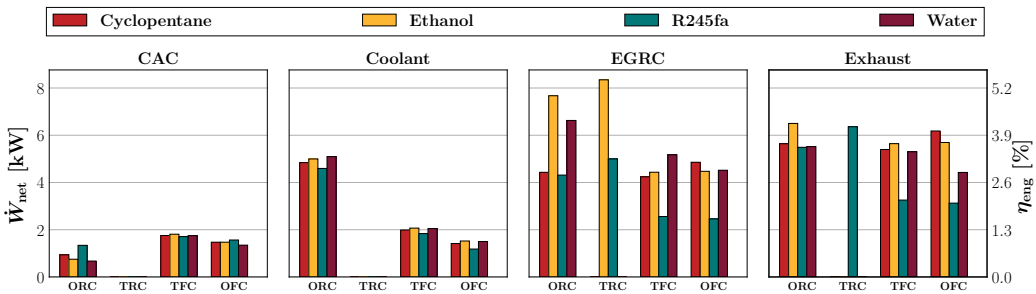

Figure 4.2: *Net produced power and the ratio of net produced power to engine power for each combination of cycle and heat source.*

4.2 Paper II

The objective of the study presented in *Paper II* was to analyze and compare thermodynamic cycles and working fluids for low- and high-temperature heat sources in a typical heavy duty Diesel engine. Over 50 working fluids were evaluated after screening based on current and future legislation. The input conditions for the cycle simulations were adjusted from those used in the previous paper to better match typical engine operating conditions and realistic cycle conditions. Because of the low energy content of the CAC at the chosen engine operating point, it was not included as a heat source.

The results for the four thermodynamic cycles - ORC, TRC, TFC, and OFC - for each selected heat source - EGRC, coolant, and exhaust - are shown in Figure 4.3. Both the ORC and TRC showed the highest power output for the EGRC and exhaust with a power output of around 2.5 kW and 5 kW, respectively. A key advantage of the ORC is that it can be operated at comparatively low pressures, so it was also suitable for WHR from the coolant, achieving a maximum power output of around 1.5 kW. The TFC offered slightly lower performance than the ORC and TRC, with maximum power outputs of around 2 kW for the EGRC, 4 kW for the exhaust, and 1 kW for the coolant. The OFC showed even lower performance, with maxima of around 1.5 kW for the EGRC, 3 kW for the exhaust, and 0.5 kW for the coolant. The best performing working fluids seemed to be acetone, cyclopentane and methanol, and to a slightly lesser extent benzene and ethanol. However, if flammability and toxicity issues of the fluids are taken into account, the best performing fluids were R1233zd(E), MM and Novec649, although in these cases, the power outputs were significantly lower than for the previously mentioned fluids.

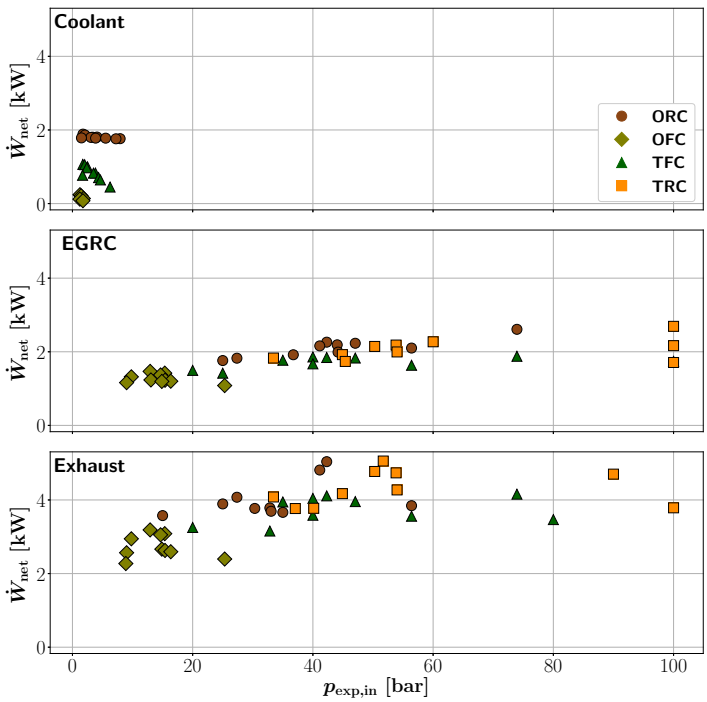

Figure 4.3: *Net produced power of the ten best performing fluids for the coolant (top), EGRC (middle), and exhaust (bottom).*

5 Discussion

The results of both papers show that the outcomes of cycle simulations depend strongly on the choice of boundary conditions and constraints. In *Paper I* the constraints were chosen to reflect optimal cycle conditions, with the goals of identifying a single optimal combination of heat source, thermodynamic cycle, and working fluid, and provide an indication of its thermodynamic potential. In *Paper II*, stricter and more realistic boundary conditions and constraints were used to evaluate WHR performance under practical engine operating conditions using known component efficiencies. The most important conditions and constraints that emerged in these studies are listed below.

Condensation temperature: A low condensation temperature makes it possible to effectively extract heat from low-temperature heat sources but also makes it difficult to reject heat to the environment. For operation in a heavy duty vehicle, the best way to efficiently use a working fluid with a low condensation temperature may be to use direct condensation instead of or in combination with a truck radiator. Additional experimental or simulation studies on heat rejection under truck driving conditions would be a valuable complement to the research presented here.

Expander efficiency: The expander efficiency, and to a lesser extent the pump efficiency, were predicted to significantly affect the thermodynamic performance of WHR systems. In both papers, these efficiencies were taken to be fixed, but in practice, the efficiency depends on the size and type of the chosen expander as well as the inlet and outlet conditions. To determine how these conditions affect WHR efficiency, more detailed expander models should be developed and used in simulations.

Max. degree of superheating: Depending on the type of fluid (wet, dry, or isentropic) and the operating conditions, allowing superheating at either the condenser or evaporator side could improve thermodynamic performance. However, excessive superheating should be avoided because it could reduce the heat transfer coefficient and increase the volume associated with the vapor flow, both of which would necessitate larger heat exchangers. Extending the heat exchanger models by incorporating correlations for heat transfer and pressure drops would allow the maximum permissible degree of superheating to be estimated.

The choice of working fluid is another important issue. A limited selection of working fluids chosen based on their performance in earlier studies was considered in *Paper I*, whereas a much larger range was considered and screened in *Paper II* on the basis of current and future legislation. However, both papers evaluated only pure fluids; no mixtures were considered. Mixtures could potentially be less flammable and/or toxic than pure fluids while offering better thermodynamic performance. Also, a number of relevant working fluid properties were completely neglected in this work. One particularly important property is the fluid's thermal stability, which determines the maximum permissible cycle temperature. Unfortunately, there is little or no reliable data on thermal stability for many fluids of interest. Other important criteria, such as material compatibility, availability and costs, should also be considered.

In both papers, each heat source was considered separately and the operating conditions of the heat sources were determined by considering a single relevant engine operating point. Including additional relevant engine operating points in the analysis would enable evaluations of thermodynamic performance in WHR over a wider spread of engine conditions. Additionally, it may be possible to improve the power output of a WHR system by combining multiple heat sources or cascading different thermodynamic cycles. Finally, the use of modified cycles incorporating new components could potentially further improve performance and power output. In particular, given suitable cycle conditions and an appropriate working fluid, the use of a recuperator could significantly improve cycle performance while also reducing the load on the condenser.

6 Conclusions and Future Work

An energy and exergy analysis of a heavy duty Diesel engine revealed that the available heat sources in the engine (CAC, EGRC, coolant and exhaust) all show potential for WHR. However, it is difficult to extract heat from the CAC and coolant because of their comparatively low temperatures. In addition, rejecting surplus heat to the environment may be as great a challenge as extracting heat from the available heat sources.

It is difficult to identify a single best combination of thermodynamic cycle and working fluid for any given heat source because WHR performance depends strongly on the applied boundary conditions and constraints, and the chosen engine operating conditions. The best results were obtained for those cycles whose temperature profiles most closely matched those of the chosen heat source. Despite the difficulty of identifying a universally optimal combination, *Paper II* showed that the ORC offered the best performance in most of the studied cases when paired with acetone, cyclopentane, or methanol as the working fluid. However, if flammability and toxicity of the fluids are taken into account, the best performing fluids were R1233zd(E), MM and Novec649.

Because the results of the simulations were highly sensitive to the applied boundary conditions, constraints, and operating conditions, it is crucial that these conditions reflect realistic engine operating conditions. Therefore, future work should include a sensitivity analysis so that the effects of the most relevant parameters on the thermodynamic cycles' power output can be reliably estimated. Also, detailed component modeling could be performed to account for several aspects that were assumed or neglected in this work. Specifically:

- A detailed expander model could be used to predict expander efficiency and performance, and to determine optimal expander sizing.
- Detailed heat exchanger models would enable estimates of heat transfer, pressure drops, and sizing.
- More detailed modeling of the thermal management of the engine, and especially engine cooling, would allow for detailed input conditions for WHR using the engine coolant as a heat source.

In addition, experimental studies will be needed to validate the modeling presented here and to get more insight into practical performance and limitations. To this end, an experimental WHR system featuring a piston expander and the exhaust as a heat source is currently under construction.

References

[1] IPCC, *Climate Change 2013: The Physical Science Basis. Contribution of Working Group I to the Fifth Assessment Report of the Intergovernmental Panel on Climate Change*. Cambridge University Press, 2013.

[2] "National emissions reported to the unfccc and to the eu greenhouse gas monitoring mechanism." `https://www.eea.europa.eu/data-and-maps/data/`. Accessed: 2018-08-02.

[3] O. Delgado, F. Rodríguez, and R. Muncrief, "Fuel Efficiency Technology in European Heavy-Duty Vehicles: Baseline and Potential for the 2020-2030 Time Frame," *The ICCT White Paper*, no. July, 2017.

[4] J. O'Connor, M. Borz, D. Ruth, J. Han, C. Paul, A. Imren, D. Haworth, J. Martin, A. Boehman, J. Li, K. Heffelfinger, S. McLaughlin, R. Morton, A. Andersson, and A. Karlsson, "Optimization of an Advanced Combustion Strategy Towards 55% BTE for the Volvo SuperTruck Program," *SAE International Journal of Engines*, vol. 10, no. 3, pp. 2017–01–0723, 2017.

[5] S. Lion, C. N. Michos, I. Vlaskos, C. Rouaud, and R. Taccani, "A review of waste heat recovery and Organic Rankine Cycles (ORC) in on-off highway vehicle Heavy Duty Diesel Engine applications," *Renewable and Sustainable Energy Reviews*, vol. 79, pp. 691–708, 2017.

[6] G. Latz, *Waste Heat Recovery from Combustion Engines based on the Rankine Cycle*. PhD thesis, Chalmers University of Technology, 2016.

[7] I. Arsie, A. Cricchio, C. Pianese, V. Ricciardi, and M. De Cesare, "Modeling and Optimization of Organic Rankine Cycle for Waste Heat Recovery in Automotive Engines," *SAE Technical Paper 2016-01-0207*, 2016.

[8] P. Petr, W. Tegethoff, and J. Köhler, "Method for designing waste heat recovery systems (WHRS) in vehicles considering optimal control," *Energy Procedia*, vol. 129, pp. 232–239, 2017.

[9] F. Yang, H. Zhang, S. Song, C. Bei, H. Wang, and E. Wang, "Thermoeconomic multi-objective optimization of an organic Rankine cycle for exhaust waste heat recovery of a diesel engine," *Energy*, vol. 93, pp. 2208–2228, 2015.

[10] S. Amicabile, J. I. Lee, and D. Kum, "A comprehensive design methodology of organic Rankine cycles for the waste heat recovery of automotive heavy-duty diesel engines," *Applied Thermal Engineering*, vol. 87, pp. 574–585, 2015.

[11] S. Edwards, J. Eitel, E. Pantow, P. Geskes, R. Lutz, and J. Tepas, "Waste Heat Recovery: The Next Challenge for Commercial Vehicle Thermomanagement," *SAE International Journal of Commercial Vehicles*, vol. 5, no. 1, pp. 2012–01–1205, 2012.

[12] G. Latz, S. Andersson, and K. Munch, "Comparison of Working Fluids in Both Subcritical and Supercritical Rankine Cycles for Waste-Heat Recovery Systems in Heavy-Duty Vehicles," *SAE Technical Paper 2012-01-1200*, 2012.

[13] J. Dickson, M. Ellis, T. Rousseau, and J. Smith, "Validation and Design of Heavy Vehicle Cooling System with Waste Heat Recovery Condenser," *SAE International Journal of Commercial Vehicles*, vol. 7, no. 2, pp. 2014–01–2339, 2014.

[14] D. T. Hountalas, G. C. Mavropoulos, C. Katsanos, and W. Knecht, "Improvement of bottoming cycle efficiency and heat rejection for HD truck applications by utilization of EGR and CAC heat," *Energy Conversion and Management*, vol. 53, no. 1, pp. 19–32, 2012.

[15] V. Macián, J. R. Serrano, V. Dolz, and J. Sánchez, "Methodology to Design a Bottoming Rankine Cycle, as a Waste Energy Recovering System in Vehicles. Study in a HDD Engine," *Applied Energy*, vol. 104, pp. 758–771, 2013.

[16] J. Bao and L. Zhao, "A review of working fluid and expander selections for organic Rankine cycle," *Renewable and Sustainable Energy Reviews*, vol. 24, pp. 325–342, 2013.

[17] H. Chen, D. Y. Goswami, and E. K. Stefanakos, "A Review of Thermodynamic Cycles and Working Fluids for the Conversion of Low-grade Heat," *Renewable and Sustainable Energy Reviews*, vol. 14, no. 9, pp. 3059–3067, 2010.

[18] S. Quoilin, M. V. D. Broek, S. Declaye, P. Dewallef, and V. Lemort, "Techno-economic survey of organic rankine cycle (ORC) systems," *Renewable and Sustainable Energy Reviews*, vol. 22, pp. 168–186, 2013.

[19] E. Macchi and M. Astolfi, *Organic Rankine Cycle (ORC) Power Systems: Technologies and Applications*. Elsevier Science, 2016.

[20] X. Dai, L. Shi, Q. An, and W. Qian, "Screening of hydrocarbons as supercritical ORCs working fluids by thermal stability," *Energy Conversion and Management*, vol. 126, pp. 632–637, 2016.

[21] S. Quoilin, S. Declaye, B. F. Tchanche, and V. Lemort, "Thermo-economic Optimization of Waste Heat Recovery Organic Rankine Cycles," *Applied Thermal Engineering*, vol. 31, no. 14-15, pp. 2885–2893, 2011.

[22] *GT-Suite, Version 7.5.0 Modified Build 1*, 2014.

[23] G. Latz, S. Andersson, and K. Munch, "Selecting an Expansion Machine for Vehicle Waste-Heat Recovery Systems Based on the Rankine Cycle," *SAE Technical Paper 2013-01-0552*, 2013.

[24] J. Szargut, D. Morris, and F. Steward, *Exergy analysis of thermal, chemical, and metallurgical processes*. Hemisphere, 1988.

[25] *Modelica language specification, Version 3.3*, 2012.

[26] *Dymola, Version 2016 FD01*, 2016.

[27] I. H. Bell, J. Wronski, S. Quoilin, and V. Lemort, "Pure and pseudo-pure fluid thermophysical property evaluation and the open-source thermophysical property library coolprop," *Industrial and Engineering Chemistry Research*, vol. 53, no. 6, pp. 2498–2508, 2014.

[28] *Python language reference, Version 2.7.13*, 2017.

[29] P. Colonna, E. Casati, C. Trapp, T. Mathijssen, J. Larjola, T. Turunen-Saaresti, and A. Uusitalo, "Organic Rankine Cycle Power Systems: From the Concept to Current Technology, Applications, and an Outlook to the Future," *Journal of Engineering for Gas Turbines and Power*, vol. 137, no. 10, p. 100801, 2015.

[30] M. Steffen, M. Löffler, and K. Schaber, "Efficiency of a new Triangle Cycle with flash evaporation in a piston engine," *Energy*, vol. 57, pp. 295–307, 2013.